Geological Survey of Canada

CURRENT RESEARCH
2005-C3

Feasibility study for using high-resolution seismic methods to estimate kimberlite deposit volumes at the Snap Lake diamond mine, Northwest Territories

D. Snyder and G. Bellefleur

2005

Natural Resources Canada
Ressources naturelles Canada

Canada

CURRENT RESEARCH

ISSN 1701-4387
Catalogue No. M44-2005/C3E-PDF
ISBN 0-662-40718-0

A copy of this publication is also available for reference by depository libraries across Canada through access to the Depository Services Program's website at http://dsp-psd.pwgsc.gc.ca

A free digital download of this publication is available from the Geological Survey of Canada Bookstore web site:

http://gsc.nrcan.gc.ca/bookstore/

Click on “Free Download”.

Toll-free (Canada and U.S.A.): 1-888-252-4301

Authors' addresses

D. Snyder (dsnyder@nrcan.gc.ca)
G. Bellefleur (gbellefl@nrcan.gc.ca)
Central Canada Division
Geological Survey of Canada
601 Booth Street, Ottawa, Ontario K1A 0E8

Publication approved by Continental Geoscience Division

Original manuscript submitted: 2005-04-28

Final version approved for publication: 2005-05-21

Feasibility study for using high-resolution seismic methods to estimate kimberlite deposit volumes at the Snap Lake diamond mine, Northwest Territories[1]

D. Snyder and G. Bellefleur

Snyder, D. and Bellefleur, G., 2005: Feasibility study for using high-resolution seismic methods to estimate kimberlite deposit volumes at the Snap Lake diamond mine, Northwest Territories; Geological Survey of Canada, Current Research 2005-C3, 11 p.

Abstract: A novel, ultra-high-resolution application of crossborehole seismology was tested at the Snap Lake diamond mine of De Beers Canada Inc. to assess whether the relatively thin kimberlite dyke that hosts the diamonds could be mapped underground with sufficient resolution to estimate accurately its volume and to guide mining. Subsequent mining and geological mapping within the test panel demonstrated that the technique was able to map the top and bottom surfaces of the dyke and to identify ramps and pinch-outs of the dyke as well as crosscutting fracture planes. In planning of the present test, De Beers Canada Inc. was advised to also trial two other geophysical methods beside the explosive sources used here. Comparison with higher frequency vibrating seismic and radar sources suggests that radar is the most effective technique in this specific application.

Résumé : Un nouvel emploi de sismique ultra-haute résolution entre forages a été mis à l'essai à la mine de diamant Snap Lake de De Beers Canada Inc. afin de déterminer si le dyke de kimberlite assez mince qui renferme les diamants pouvait être cartographié sous terre avec suffisamment de résolution pour permettre une bonne estimation volumétrique et guider l'exploitation souterraine. L'exploitation et la cartographie géologique de la zone mise à l'essai, effectuées par après, ont démontré que cette technique permettait de cartographier les surfaces supérieure et inférieure du dyke, ainsi que de reconnaître les rampes et les terminaisons en biseau du dyke et les plans de fractures recoupant le dyke. Durant la planification de cet essai de sismique à source explosive, nous avons conseillé à De Beers Canada Inc. de mettre à l'essai deux autres méthodes géophysiques utilisant des sources différentes. La comparaison de nos résultats avec ceux obtenus à l'aide de sources sismiques vibratoires à haute fréquence et radar suggère que la méthode au radar est la plus efficace pour cet usage particulier.

[1] Contribution to ESS Ventures Project

PURPOSE OF SURVEY AND SETTING

This survey was undertaken in the Snap Lake underground project of De Beers Canada Inc. in order to assess whether accurate remote mapping of the target kimberlite dyke could be achieved by geophysical methods in order to guide the actual mining of the ore. Three independent geophysical investigations were conducted in successive weeks over a target test panel approximately 50 m by 70 m. This paper describes the third of these surveys, a seismic crosshole survey using explosive energy sources. A map of the hanging wall of the kimberlite dyke is the output sought. This was achieved although multiple dykes, ramps, and pinch-outs were also detected and mapped. Ground Penetrating Radar (GPR) and vibroseis surveys provided higher resolution 2-D sections of the dyke, but none of the techniques has met all hopes and expectations for mining application.

Snap Lake is located within the southern part of the Slave Craton, about 220 km east-northeast of Yellowknife, Northwest Territories, Canada (Fig. 1). The kimberlite dyke is emplaced primarily within granitic rocks of the Defeat suite (2610–2590 Ma) (Bleeker et al., 1999), but outcrops within mafic metavolcanic and metaturbidite rocks of a greenstone belt (Kirkley et al., 2003). The hypabyssal kimberlite dyke is unusual in its near-horizontal attitude and its high proportion of coarse-grained macrocrysts (3–10 mm crystals) (Kirkley et al., 1991, 2003); many (2 carats/t) of these macrocrysts are high-quality diamonds. Drilling and a surface seismic reflection survey (Hammer et al., 2004) have shown the dyke to dip at approximately 15°NW, but locally ranges from 5°–30°. It is complex in form, occasionally feathering into multiple strands or rapidly changing dip.

Physical-property measurements were made on drill core of both kimberlite and host rocks at Snap Lake (Hammer et al., 2004). Kimberlite samples averaged 4.3 ± 0.1 km/s at 50 MPa pressure. Host-rock samples averaged 5.6 ± 0.2 km/s at 50 MPa pressure. Densities were 2.40–2.49 g/cm^3 versus 2.66–2.95 g/cm^3, respectively. These properties plus synthetic seismic modelling demonstrate that the dyke should be reflective to seismic waves typically used in exploration (Hammer et al., 2004).

ACQUISITION: 6–13 SEPTEMBER 2004

In-mine acquisition

Acquisition of the seismic data used four, nearly horizontal (1.1° < average dip < 3.3°) holes that were accessed from a single drilling cubby located about 180 m below the surface of Snap Lake. All four holes were NQ size (7.53 cm diameter), drilled into granitic rocks. Fractures that produced water were all grouted and redrilled, so that the shafts were very smooth.

Receivers

Previous groups had installed pulleys and 100-pound-test strings in each hole and these proved indispensable for inserting the receivers into the holes. Trial attempts showed that manual insertion would not work reliably without mechanical assistance of some kind. The receivers were an eight-element chain of three-component (orthogonal) seismometers manufactured by Vibrometrics™. Each set of three components was spaced 10 m apart and had a retractable clamping arm. The last set was placed 2.0–2.5 m from the drillhole collar to limit the amount of lead-in cable going to the

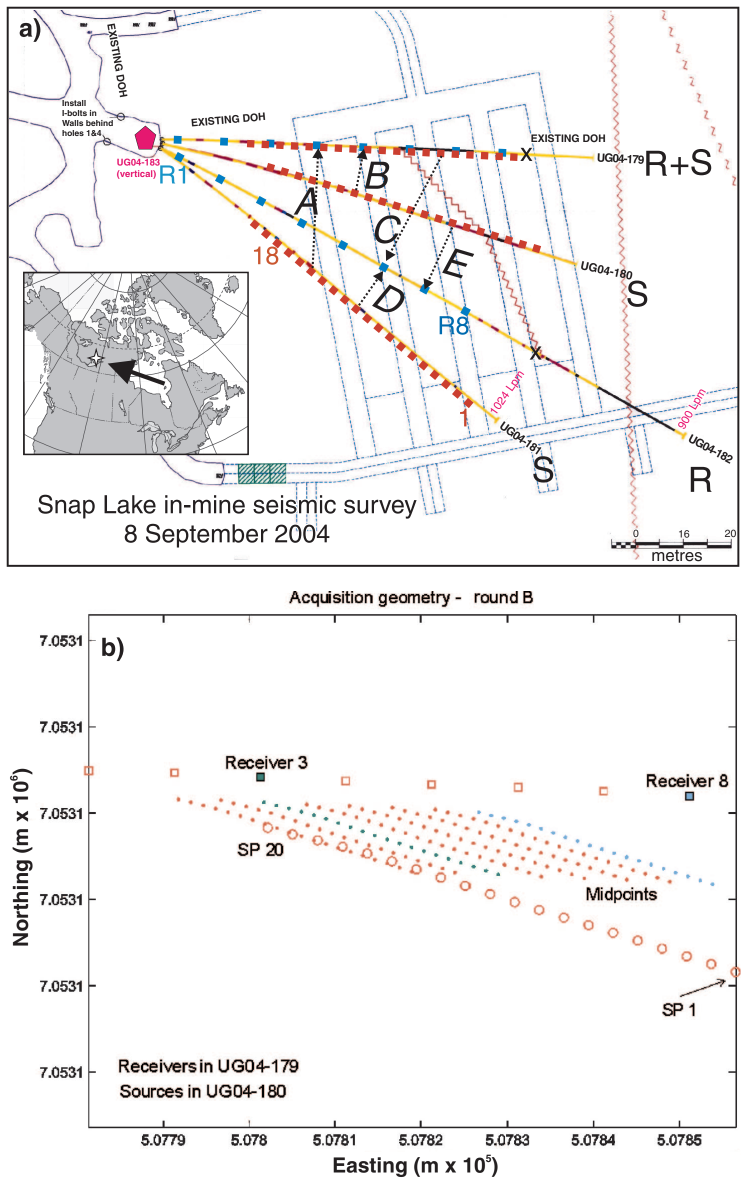

*Figure 1. Acquisition geometries: **a)** Map showing rounds A–E that comprised the entire survey using eight receivers (R) and 18 or 20 sources (S) in five pairs of drillholes. **b)** Midpoint map for round B only. Note that radiating hole pattern causes all midpoints to be offset different amounts to form a low-fold, but uniform coverage, here with about 1.5 m spacing between midpoints.*

Geometrics Geode™ seismic acquisition system. Early testing showed that longer cables picked up considerable 60 Hz noise from the underground electrical circuits. Receivers were placed in holes UG-04-179 and UG-04-182 (Fig. 1).

Sources

Previous studies in Switzerland led the authors to choose small explosive sources (single detonators) as the preferred seismic wave source (Bühnemann and Holliger, 1998). Zero-delay detonators taped onto a flexible, nonstatic loading hose at 3 m intervals provided the energy source. Shots were fired in rounds of 18–20 in a single shot hole using a separate lead for each shot point. Each source was then detonated using a custom blast box synchronized to a twin that sent a simultaneous trigger to the acquisition system. Three holes were used as source locations (Table 1) during five rounds of shots. In at least two of the holes, detonators broke the pulley lines and made subsequent use of those holes for receivers impractical.

Shooting schedule

Data were acquired over two days after two days of layout and start-up tests. Layout included testing of the pulley system for the receivers, design and wiring the leads for the shooting string, and transporting all the equipment into the mine. Start-up testing was primarily to determine proper signal-to-noise ratios. This included characterization of the many sources of noise in the mine and trials with single or double detonator charges. The in-mine radio system apparently caused sufficient noise on the trigger cable or else internal cross-feed within the blasting box caused random self-triggering of the recording system. This was avoided by using synchronized trigger boxes for the detonator and recorder. Single detonators were deemed sufficient if all machines operating in the lower mine level were turned off and a 'quiet' period enforced during shooting. Each round took 20–30 minutes. During the shooting of the five rounds of seismic data described here, an estimated 3–4 hours of mining operations were lost over the two days. Quiet periods were co-ordinated where possible so that haul trucks were unloading ore at the surface during these periods.

Preprocessing of data

The initial processing step was application of the source-receiver geometries to each seismic trace using drillhole deviations derived from geodetic surveys of the collar and EZ-Shot™ downhole measurements. These two survey methods did not match well initially, but this was resolved by a few additional measurements near the collar. Spectra of the recorded signal indicate that useful seismic energy was recorded from about 80 Hz to 5000 Hz with a peak between about 1000 Hz and 2500 Hz, so the data were bandpass filtered to retain frequencies between 200 Hz and 3500 Hz. The large receiver spacing means that tube waves are spatially aliased, but these waves were only rarely observed. After filtering, 'P' direct waves are clearly observed on shot and receiver gather records, some direct S-waves, and reflections from reflector planes both parallel to the hole and intersecting it at high angles.

Analysis of first-break arrivals at two receivers that are in-line with a round of sources showed time versus offset distance indicating velocities of 5555 m/s and 5843 m/s in the 'granite'. Assuming a central frequency of about 2800 Hz, these velocities indicate a nominal seismic wavelength of about 2 m. Standard resolution criteria suggest that these waves should resolve structures 50 cm or less in thickness. The observed time of the first arrival of 8.5 ms was about double that expected from the 22 m near-offset and suggests that the shot and trigger clocks were not completely synchronized; this delay can be treated as a predictable static shift.

The data were initially studied as common shot gathers (field records) with eight traces per gather. More traces enable better picking of significant arrivals, so data sorted into common receiver gathers with 18–20 traces each (Fig. 2) were sufficient to identify phases for preliminary interpretation. The data from different rounds were next sorted with respect to the midpoint between source and receiver (Fig. 1b). Using the constant velocities determined from first-break analysis, normal moveout due to variable offsets can be removed to produce 'zero-offset' sections, or eventually 3-D maps of reflector surfaces in the region where common midpoints occur.

Description of field-data records

Common receiver gathers provide a quick, preliminary assessment of the data quality and allow some simplistic calculations of travel paths and interpretation of reflector depths or attitudes. The displays used are grouped into the three orthogonal traces recorded at one location for all 18 or 20 shots fired during one round (Fig. 2). In each case, the minimum travel time for the first arrival occurs where the source was closest to the receiver, the minimum offset. Greater travel times indicate greater offsets and it is these variations

Table 1. Source and receiver locations in boreholes.

Round	Source hole	Source offsets (metres from collar)	Receiver hole	Receiver offsets (metres from collar)
A	UG-04-181	83–32 by 3 (18)	UG-04-179	2.5–72.5 by 10 (8)
B	UG-04-180	81–24 by 3 (20)	UG-04-179	2.0–72.0 by 10 (8)
C	UG-04-179	75–18 by 3 (20)	UG-04-182	2.0–72.0 by 10 (8)
D	UG-04-181	81–24 by 3 (20)	UG-04-182	2.0–72.0 by 10 (8)
E	UG-04-180	81–24 by 3 (20)	UG-04-182	2.0–72.0 by 10 (8)

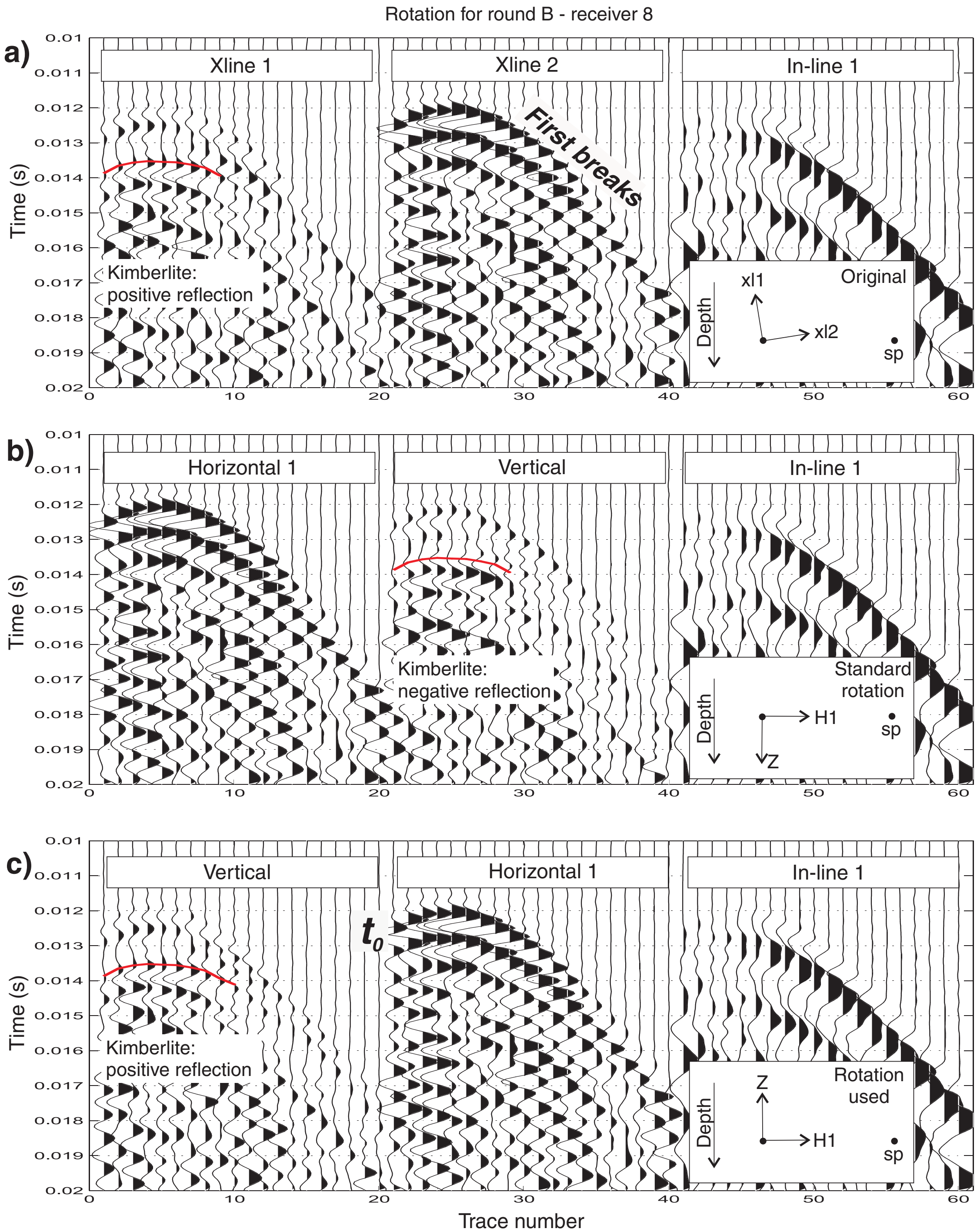

***Figure 2.** Three-component data examples: receiver gathers of round B, receiver 8. **a)** Original, in-line and two randomly oriented cross-line components showing clear first-break arrivals and several secondary (presumably reflection) arrivals. Inset shows probable orientation of two crossline components in cross-sectional view. **b)** Crossline components synthetically rotated so as to maximize first-break energy on the first component and make it the horizontal component (*see *inset). The second component is then oriented vertically and reflections from below appear primarily on this component. **c)** Alternative rotation of the crossline components so as to maximize first break (t_0) energy on the second component and make the other component point vertically and upward (inset), making reflections from kimberlites appear as positive 'wiggles'.*

that can be removed by applying a normal move-out correction that accounts for this increasing offset between source and receiver. This move-out typically appears as a hyperbolic line of similar arrivals. Later hyperbolic curves indicate reflections from planar surfaces below or parallel to the line of shots. Dipping, diagonal phases usually indicate reflections from planes intersecting the drillhole at high angles. Both are observed on the common receiver gathers from this survey. In this geological setting, kimberlite dykes and fracture zones are the most logical reflectors, respectively.

Delay times between the hyperbolic curves marking first arrivals and secondary ones can be used to estimate the depth to reflectors beneath the geometrical plane containing the sources and receivers. This was done for eight receiver gathers that showed particularly clear secondary arrivals on one or more components. Because nearly constant seismic wave speeds occur in the granite, linear travel paths can be assumed. Because the target dyke is parallel to the boreholes, knowing only the source-receiver offset allows each observed delay to be converted into a depth estimate (Table 2). Assuming that offsets were surveyed accurately, uncertainties arise primarily from variations in wave speed within the volume of the survey area and in measuring the delay time. Wave speeds appear to vary by ±150 m/s. Delay times were picked with about 5% uncertainty. For example, assuming a wave speed of 5845 m/s instead of 5555 m/s increased the depth estimate for round E, receiver location 7 (E:R7) from 10.12 m to 10.45 m. In general, estimated depths are accurate to 10% or better. Some obvious wave-speed decreases are observed near logged fracture zones and these delay arrivals and increase the apparent depth of reflectors.

Summary of acquisition

Analysis of the frequencies recorded suggests potential resolution of structures about 0.5 m thick. Quieting of all nonessential machinery in the mine during recording is critical to good signal observation.

1) Clear, consistent direct arrivals can be seen throughout all surveys and these indicate a homogenous background medium of granitic rock, with the possible notable exception of low-velocity zones associated with fracture and fault zones.
2) Multiple reflections follow these first arrivals at most locations indicating reflections from planes, probably above or below the drillholes. The only known, probable candidate for such reflectors is the kimberlite dyke, as mapped in the mine and detected from surface seismic surveys.
3) Simplistic estimates of the depth of reflectors beneath the plane defined by the four surveyed drillholes at eight locations indicates one at 8–10 m and another 4 m deeper. Uncertainty is about 50 cm.
4) In some areas the reflected signal is weak to nonexistent and this may indicate local variation in reflector thickness, perhaps a zone of pinching, swelling, or fingering of dykelets.
5) Joint analysis of all five surveys will provide a map of the reflector surfaces for the area between the drillholes located 10–80 m from the collars with an average spatial density of a few metres.
6) A few high-angle reflectors were also detected. These appear to correlate with known fracture zones, but the attitude of the plane over an area of tens of square metres can be estimated from the reflection pattern.

PROCESSING

After acquisition, each round of data was inspected for quality. A weak X or Y component on receiver levels 4 and 5 meant that these levels could not be used for further analysis that required all three components. The acquisition geometries, while maximizing the area with single-fold coverage (Fig. 1b) also meant that shot gathers for receiver levels 1–3 had reflected arrivals nearly coincident with direct arrivals. Efforts were therefore directed to using receivers 6–8 for each of the five shooting rounds A–E. The desire to maximize spatial resolution resulted in use of a pass band of 250–2500 Hz.

Rotations

One important processing step takes advantage of the three components recorded, albeit in an unknown, arbitrary orientation during acquisition. During processing the components can be synthetically 'rotated' so that one appears to point vertically and another points back toward the seismic source. In general, the component 'in-line' with the axis of the recording drillhole had markedly lower frequency content (Fig. 2a) and was excluded from the rotation analysis. Because source and receiver holes were at almost the same elevation, direct seismic waves will appear mostly on the horizontal component, whereas seismic waves reflected from below will be

Table 2. Preliminary depth estimates to reflectors (t_0 is first-break time; t_1, t_2 are reflection arrival times).

Round	Offset (m)	t_0 (ms)	t_1 (ms)	t_2 (ms)	Delay 1 (ms)	Delay 2 (ms)	Depth 1 (m)	Depth 2 (m)
A:R7	38.9	14.3	16.7	18.2	2.4	3.9	17.4	23.2
B:R7	15.0	11.4	13.0	14.4	1.6	3.0	9.7	14.2
C:R6	25.5	12.8	13.9	15.0	1.1	2.2	9.3	13.9
C:R8	34.5	14.4	15.7	17.4	1.3	3.0	11.7	18.9
D:R5	7.4	9.4	10.3	11.9	0.9	2.5	1.4	10.0
E:R3	7.0	9.5	11.3	12.6	1.8	3.1	7.7	11.6
E:R7	15.5	11.1	12.9	13.3	1.8	2.2	10.1	11.5

recorded mostly on the vertical component (Fig. 2b). By searching for the pair of orientations that maximize the first breaks (t_0) on the horizontal component, reflected energy of interest to this study can be isolated on the vertical component. The standard display convention is that vertical down is positive (black), so that seismic waves reflecting off a step increase in velocity below the borehole would appear as a positive wiggle. Instead, the authors choose vertical up to be displayed as positive on the vertical component and a negative velocity and/or density contrast below the drillhole, such as a kimberlite dyke, then produces a positive wiggle (Fig. 2c).

Analysis and interpretation

Records for seismometer levels 6–8 in each of rounds A, B, C, and E were processed in this way and then analyzed for possible reflections from the kimberlite dyke. Most records showed several good reflections that could come from either above or below the borehole. Because physical-property studies and the previous surface seismic survey (Hammer et al., 2004) indicated that the kimberlite represented a strong, negative velocity contrast and impedance contrast, the present authors sought high-amplitude and laterally continuous, positive-polarity seismic phases corresponding to reflections located 5–15 m below the borehole. Formal and precise migration of the data cannot be performed with the DSISoft processing code used in this analysis. A process called "CDP transform" in DSISoft could do this migration if one assumes that the kimberlite is a planar surface, however, the distribution of midpoints is probably too sparse to properly reconstruct an image from constructive interference. Therefore theoretical traveltime curves corresponding to depths of 8 m, 10 m, and 12 m help guide the picking of reflected seismic-wave arrivals. These guides roughly match the first reflections following the direct arrivals. The picked times of a deeper set of reflections were also analyzed and used to produce an elevation surface. Both reflection sets were noted during the acquisition of the data.

Seismic velocities in rocks located between the acquisition holes and target reflector strongly influence the traveltime arrivals. The first-break arrival times were inverted in a 2-D P-wave tomography study within the plane defined by the acquisition boreholes using all first breaks available (Fig. 3). P-wave velocities vary from 5700 m/s to 5950 m/s, consistent with earlier determinations of 5850 m/s made using a single receiver gather (round B1 in Fig. 1). A velocity of 5850 m/s was used for quick depth estimates and the 2-D velocity model for final estimates. Observed static shifts associated with individual receivers or shots can be attributed to 1) small timing errors between shot and recorder triggers, 2) poor coupling of a receiver in the borehole, or 3) unusual rock properties (fractures or cavities) near a shot or receiver. These static shifts were added to first breaks to produce more accurate 2-D velocity models and more accurate reflector depth estimates.

Reflector depths were estimated by calculating the difference in observed traveltime between a direct (horizontal) arrival and a seismic wave bouncing off a layer below (or above) the plane of boreholes, attributing that delay solely to additional path length. Simple trigonometry requires that the horizontal offset (x) between source and receiver, the time delay (t in Fig. 4) and the velocity (v) be known to calculate the reflector depth (z):

$$z^2 = 0.25\,[(vt)^2 - x^2]$$

It can be assumed here that the reflector is nearly planar and subhorizontal. Velocities obtained from first-arrival traveltimes (Fig. 3) were used to calculate the depth of the reflections for each source-receiver pair.

Not all shot-receiver pairs provide a clear reflection with which to estimate the reflector depth. The midpoint reflection point of those pairs producing estimates were mapped with respect to the drillholes (Fig. 5) and hence to mine coordinates. Figure 5 shows locations of midpoints and elevations estimated for the deeper set of reflections. This set likely corresponds to the hanging wall of the kimberlite. Some picks were re-examined to make them more internally consistent where midpoints coincided. Reflector elevations range from 5254 m in the southwest to 5268 m in the northeast. These midpoint determinations can be contoured and smoothed (Fig. 6) and then compared with contoured plots of hanging-wall depths as determined by subsequent mining of the test panel (Fig. 7). Comparison of the seismic and geologically mapped hanging-wall surfaces must be done with care as differences can result from interpolation effects (the two surfaces are not constructed from coincident points). Where well constrained the discrepancies are generally less than ± 2 m. Maximum discrepancies are ± 5 m in three areas. In these areas multiple reflections are observed (Fig. 4) and the kimberlite dyke may have several splays. Therefore the same surface is not being mapped by these two different survey methods.

Interpretation

Neither the reflection sections from each receiver gather studied (e.g. Fig. 4) nor the composite map to reflector depth (Fig. 6) indicates that the kimberlite dyke has planar, single-layer geometry within the test panel. Ramps, pinchings, swellings, and areas with stacked splays are indicated; one ramp appears consistently on over half of the receiver gathers studied (Fig. 5). For dykes thicker than 3 m the authors' method can resolve both the hanging wall and footwall, nominally as a positive-negative 'wiggle' pair separated by about 0.5–1.5 ms depending on offset (Fig. 4).

Interpretation is seldom straightforward due to multiple prominent, and sometimes interfering, reflections present. On the example shown in Figure 4 and on other receiver gathers, typically three strong reflectors are observed. These generally coincide with depths of 5 m, 10–14 m, and 19 m although amplitudes vary considerably and ramps link the various levels. For example, on receiver gather B6 (Fig. 4), it is the 14 m reflector that is contoured on the eastern half of the section and the prominent, 10 m one on the western half. These two levels appear to overlap between traces 9–13 and the prominent 10 m reflector appears to ramp down from about 7.5 m depth at trace 9 to 18–20 m depths at traces 18–20

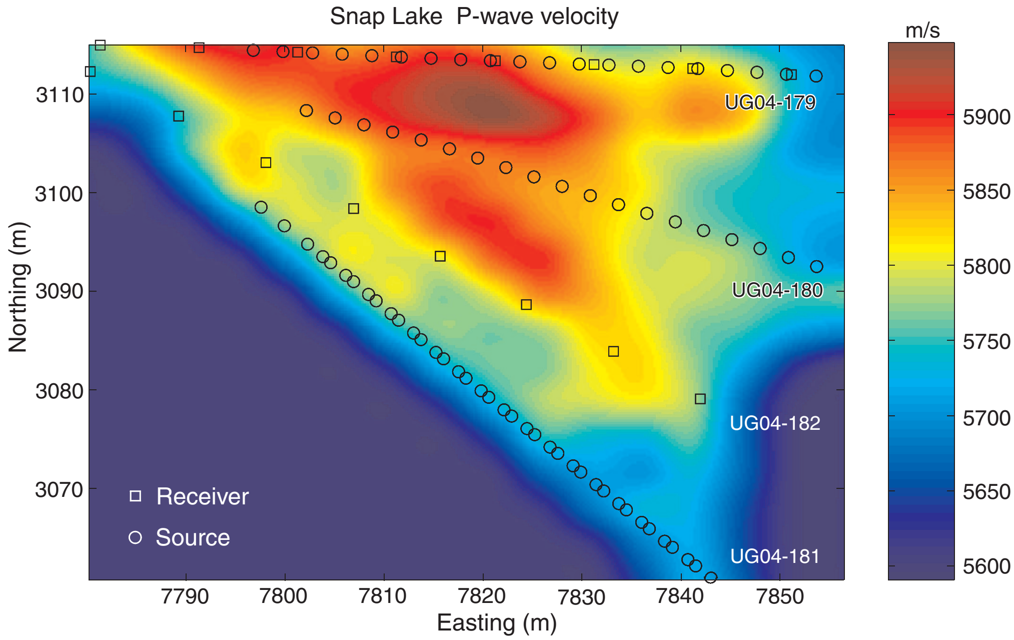

Figure 3. P-wave velocity map in the plane of the acquisition boreholes. This 2-D tomographic inversion used all first-break arrivals from all five rounds recorded and therefore provides meaningful values only between the four boreholes (i.e. ignore velocities <5700 m/s).

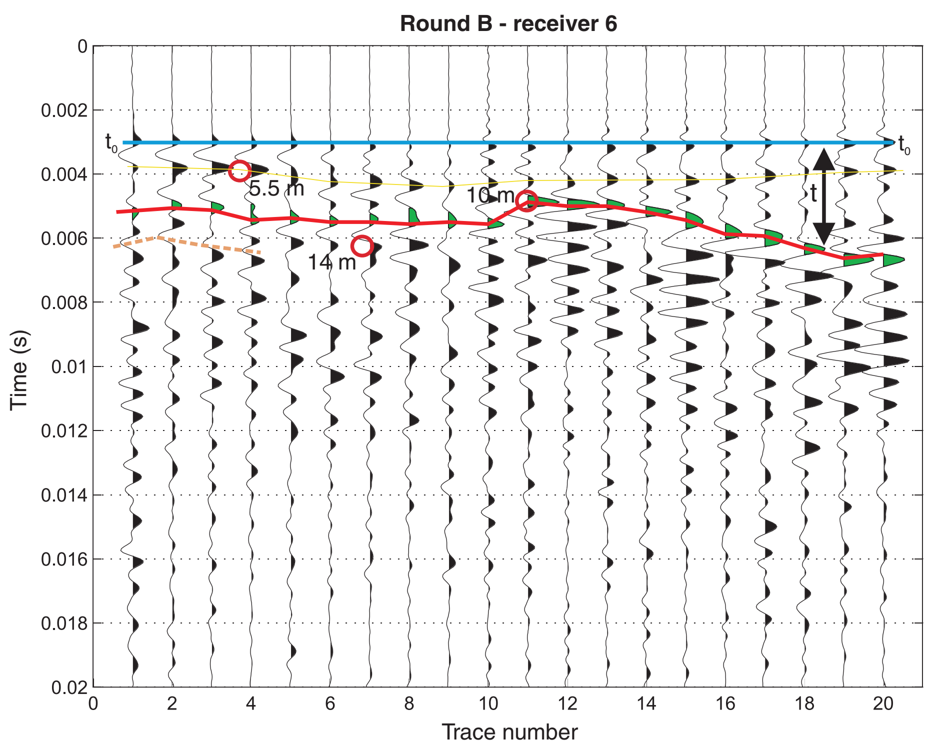

Figure 4. *Example of a receiver gather (round B, receiver 6) with all first breaks (t_0) shifted to the same time. This corrects for differences in offset between sources and receivers and better allows comparison of possible reflections by reducing hyperbolic moveout of secondary seismic phase arrivals. The delay between first break and reflection arrival (t) is used to calculate the depth to a planar reflection. Here the solid line shows the arrival picks for a possible reflector at 10–14 m, although several depth estimates are indicated by circles. Lateral continuity of high amplitude and similar-shaped wiggles are the guide, but few clear reflections appear across the entire gather. The parallel dashed line on traces 1–4 indicates possible reflections from the bottom of the picked kimberlite dyke; it is about 3 m thick.*

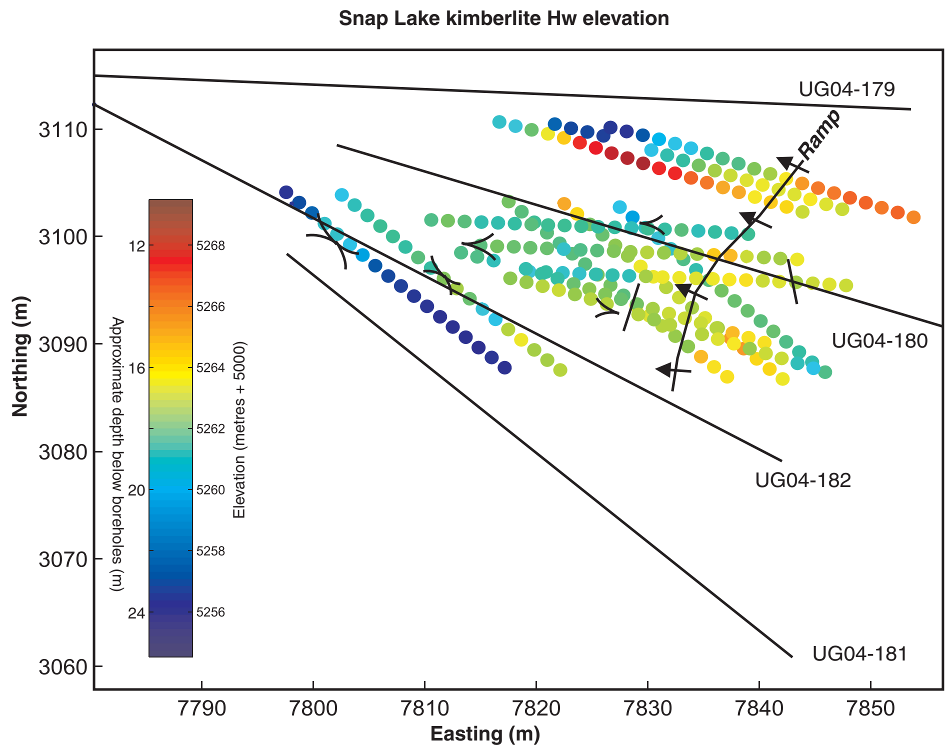

Figure 5. *Map of midpoint locations where depth estimates to the top (hanging wall) of at least one kimberlite dyke were possible in rounds A2, A3, A6–A8, B6–B8, C6–C8, and E6–E7. Elevations are in metres above sea level plus 5000 m. If assumed to represent the same surface everywhere, the surface has over 10 m of vertical relief within the area of the seismic survey, but concentrated mostly in the north. Inferred structures include a prominent ramp (arrows point downdip), mergings of two dykes into one (< and > symbols) and truncations by faults (line segment).*

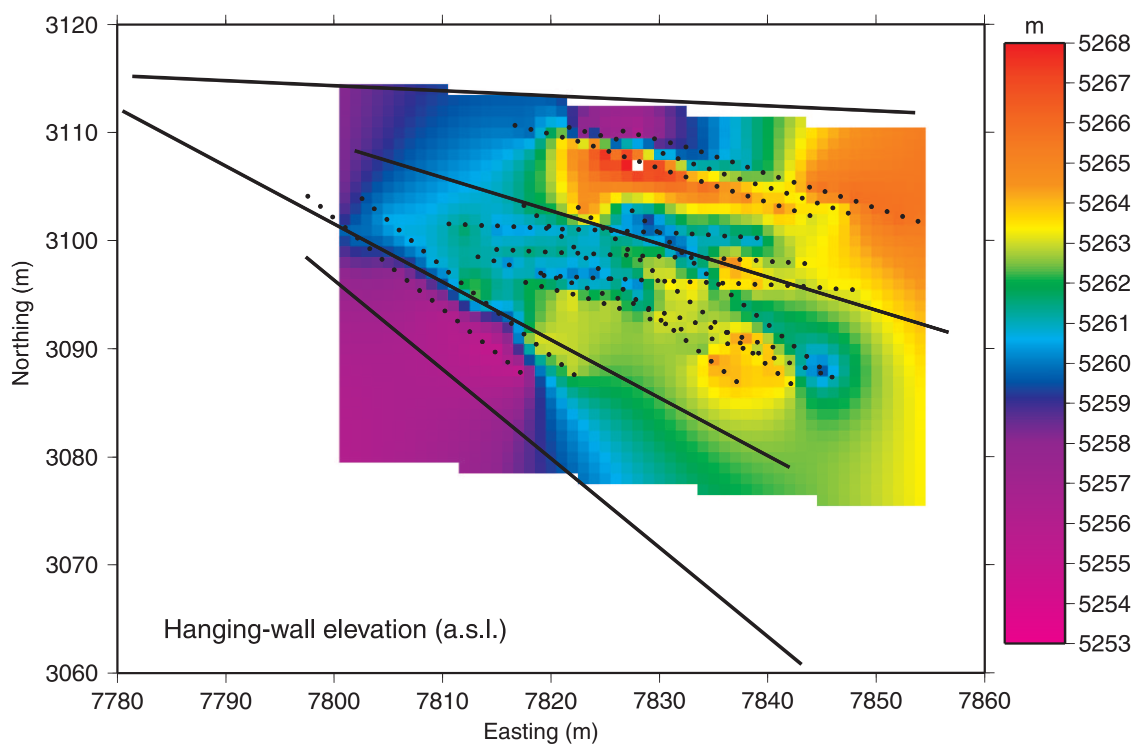

Figure 6. *Contoured and smoothed version of Figure 5.*

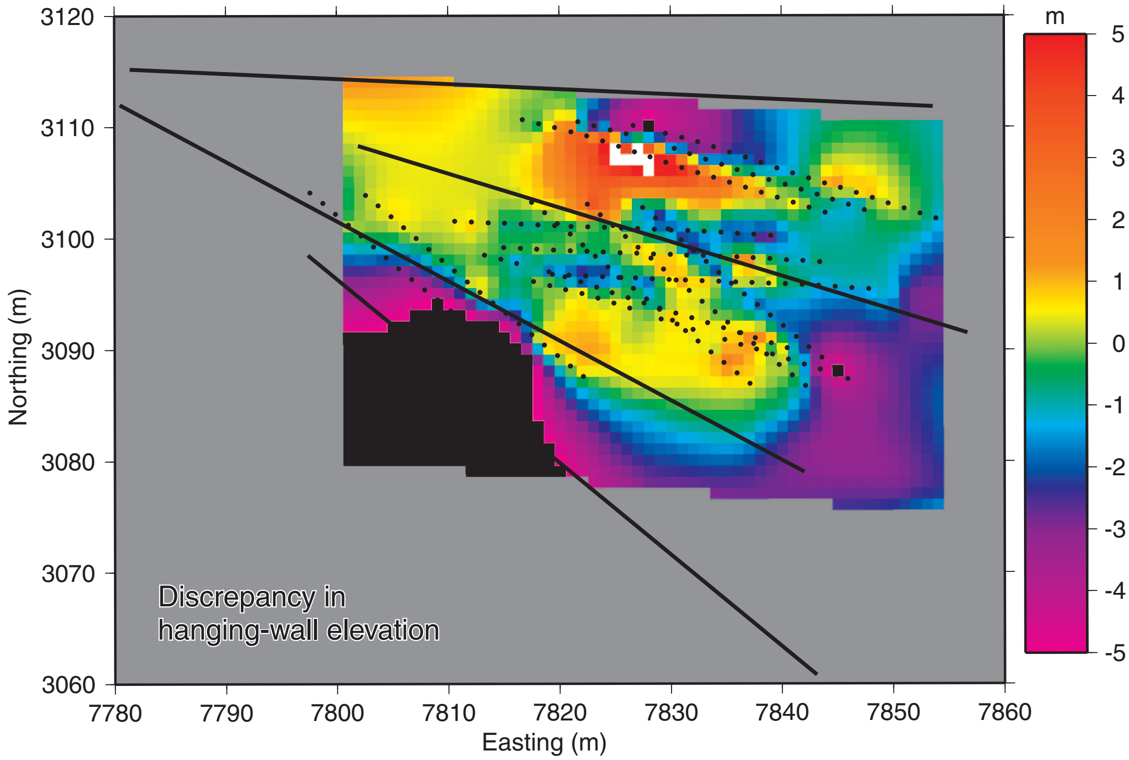

Figure 7. Map of depth discrepancies between the seismic estimates discussed here and elevations of the hanging wall as mapped geologically in the walls of mine tunnels within the test panel. The midpoints do not coincide with the tunnel mapping locations so that two independent contour maps were subtracted to get these values. Where well constrained the discrepancies are generally less than ±2 m. Multiple dyke splays and hanging-wall surfaces are indicated in the seismic data and may account for some larger discrepancies.

(Fig. 4, 5). Although improbable because of its nonplanar shape, this prominent reflector could also represent a steeply dipping fracture plane.

Other reflections also do not display theoretical hyperbolic shapes that would originate from planar reflectors parallel to the plane of acquisition; these probably represent reflections from subvertical fracture planes that intersect the acquisition holes (Fig. 8). Reflections from above the boreholes can also not be eliminated completely although few if any sizable (mafic) dykes with seismic velocities greater than the host granitic rock have been observed in the mine. Note that positive velocity contrasts are required above the acquisition boreholes in order to mimic negative contrasts observed below the holes.

Conclusions

Two, possibly three, laterally extensive kimberlite dykes can be inferred from three lateral continuous reflector surfaces with seismic characteristics appropriate for the Snap Lake kimberlite. These are generally located at depths of 6 m, 10–14 m, and 19–21 m. The deepest surface, on average, coincides within ±2 m with a kimberlite mapped within the mine. Reflection amplitudes indicate that this is not necessarily the thickest dyke everywhere within the test panel. A few steeply dipping fracture planes are also inferred from seismic reflections.

ASSESSMENT AND APPLICATIONS TO MINING

A surprising amount of information can be extracted from borehole seismic data. The interpretation of multiple dykes as well as the ramps and splits are consistent with the interpretations drawn from the radar and swept impact seismic surveys. All geophysical interpretations correlate well with current understanding and knowledge of the dyke as mined in the test-panel area. Drilling intersected a second dyke, approximately 5 m above the main dyke exposed in the test panel. The drilling intersection confirms the interpretations indicating that the dyke splits into two splays. Discrepancies in the elevations between the dyke horizons mapped by the geophysical techniques and exposed by mining activities are mainly attributed to sparse mapping of multiple horizons. The horizons tracked in the geophysical interpretations do not necessarily coincide with the horizon currently being

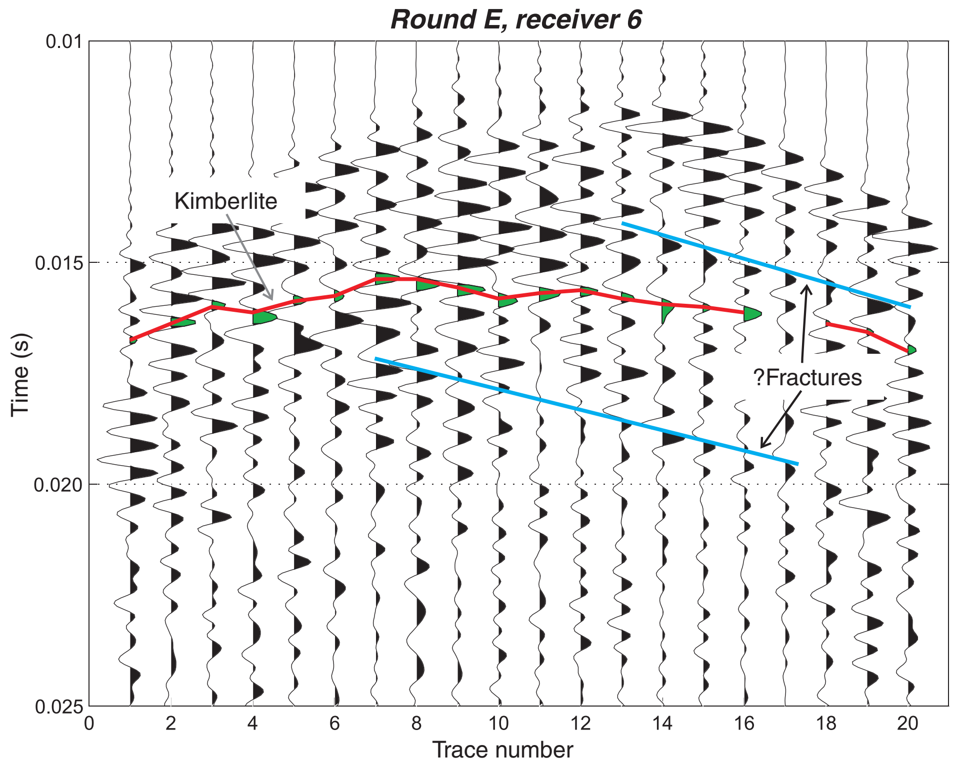

Figure 8. *Example of a receiver gather from round E, receiver 6. Unlike Figure 4, this gather has no time shifts. Solid line shows picks for hanging-wall surface. Straight lines show alignments of seismic waves that do not have typical hyperbolic moveout associated with reflections from above; their straight alignments suggest reflections from fracture planes at high angles to the plane of acquisition boreholes and intersecting hole UG04-180 at about shotpoint 6.*

mined. The greatest concern from a mining perspective, and the geophysical interpretations allude to this, is that mining may not be tracking the thickest dyke horizon.

Mapping of actual dyke thickness from borehole scanning techniques has the potential to make a major contribution to resource evaluation and mining. The main drawback is the minimum thickness limit imposed by the seismic wavelength used here. The mapping or detection of fractures or faults that are not intersected by the boreholes is very valuable additional information. It assists with understanding the structural controls and is also obviously a good early warning system for potential geotechnical or hydrological hazards to be encountered by mining.

Out of the three geophysical methods tested, in this specific environment, the radar offers the best solution. Logistically it is the easiest to manage and deploy with very short data acquisition times. Data resolution is the highest of the techniques, with very wide coverage over the survey area. One of the main problems for the seismic techniques was the very wide angle of reflection caused by the relatively large source-receiver offset with respect to the distance of the boreholes to the dyke. Sources and receivers deployed in parallel or orthogonal holes rather than the radiating pattern used here could provide small angles of reflection, but would increase drilling costs. The near coincident source-receiver geometry of the radar instruments when used in single-hole configuration circumvents many of these problems.

The results of the three techniques correlated well. All the techniques indicated multiple dyke horizons with interpretations showing the main dyke ramping and splaying into two dykes over the test-panel area. The data density obtained from the radar and swept-impact seismic applications facilitates the accurate tracking of the horizons and makes it easier to resolve the complex geology. One of the drawbacks of the radar (as opposed to seismic techniques) is the high attenuation of the EM wave in the kimberlite. It therefore becomes increasingly difficult to detect reflections from a second dyke as the thickness of the dyke above it increases.

The borehole scanning techniques have not had any impact on actual long- or medium-term mine design at this stage. It does provide a good guidance system for directing active development in mainly two applications: 1) to guide development and provide early warning of ramping and splitting of the dyke, and 2) as a tactical tool to detect the dyke once development 'lost' the dyke.

ACKNOWLEDGMENTS

M. Kirkley, D. McBean, and A. Wohlmarens of De Beers Canada Inc. provided support and assessments of the project's utility throughout. Other De Beers Canada Inc. staff at the Snap Lake mine site provided key aid during the acquisition.

REFERENCES

Bleeker, W., Ketchum, J.W.F., Jackson, V.A., and Villeneuve, M.
1999: The Central Slave Basement Complex, Part I: its structural topology and authochthonous cover; Canadian Journal of Earth Sciences, v. 36, p. 1083–1109.

Bühnemann, J. and Holliger, K.
1998: Comparison of high-frequency seismic sources at the Grimsel test site, central Alps, Switzerland; Geophysics, v. 63, p. 1363–1370.

Hammer, P.T.C., Clowes, R.M., and Ramachandran, K.
2004: Case history: high-resolution seismic reflection imaging of a thin, diamondiferous kimberlite dyke; Geophysics, v. 69, p. 1143–1154.

Kirkley, M.B., Gurney, J.J., and Levinson, A.A.
1991: Age, origin and emplacement of diamonds: scientific advances in the last decade; Gems and Gemology, v. 27, p. 2–25.

Kirkley, M.B., Mogg, T., and McBean, D.A.
2003: Snap Lake Trip Guide; *in* 8th International Kimberlite Conference, 2003 Field Trip Guidebooks (Slave Province and Northern Alberta), (ed.) B.A. Kjarsgaard; Geological Survey of Canada, Miscellaneous G, 293 p. 67–78.

Geological Survey of Canada RC200-303510